IOPscience iopscience.iop.org

Home Search Collections Journals About Contact us My IOPscience

Similarity of fluctuations in systems exhibiting Self-Organized Criticality

This article has been downloaded from IOPscience. Please scroll down to see the full text article.

2011 EPL 96 28006

(http://iopscience.iop.org/0295-5075/96/2/28006)

View the table of contents for this issue, or go to the journal homepage for more

Download details:
IP Address: 195.134.94.87
The article was downloaded on 06/10/2011 at 07:42

Please note that terms and conditions apply.

A Letters Journal Exploring the Frontiers of Physics

October 2011

EPL, **96** (2011) 28006 www.epljournal.org
doi: 10.1209/0295-5075/96/28006

Similarity of fluctuations in systems exhibiting Self-Organized Criticality

N. V. Sarlis, E. S. Skordas and P. A. Varotsos[(a)]

Solid State Section and Solid Earth Physics Institute, Physics Department, University of Athens Panepistimiopolis, Zografos 157 84, Athens, Greece, EU

received 28 June 2011; accepted 1 September 2011
published online 5 October 2011

PACS 89.75.Da – Systems obeying scaling laws
PACS 95.75.Wx – Time series analysis, time variability
PACS 91.30.Ab – Theory and modeling, computational seismology

Abstract – The time-series of avalanches in three systems exhibiting SOC are analyzed in natural time χ. In two of them, *i.e.*, ricepiles and magnetic flux penetration in thin films of $YBa_2Cu_3O_{7-x}$, the data come from laboratory measurements, while the third one is a deterministic model mimicking stick-slip phenomena. We show that their scaled distributions for the variance κ_1 of natural time exhibit an exponential tail as previously found for the order parameter in seismicity and in other non-equilibrium or equilibrium critical systems. Upon considering the entropy S_- in natural time under time reversal, the following important difference is found: In ricepiles evolving to the critical state, S_- is systematically larger than the entropy S in natural time, while in $YBa_2Cu_3O_{7-x}$ no systematic difference between S_- and S is found.

Copyright © EPLA, 2011

Introduction. – During the last decade, a new time domain, called natural time χ, has been introduced [1] which has been shown [2] to be optimal for enhancing the signals' localization in time-frequency space, thus reflecting that natural time reduces uncertainty and extracts signal information as much as possible. Natural time analysis (see below) has been applied to diverse complex time-series like electrocardiograms [3–5], ion currents fluctuations in biological membrane channels [1,6], the statistical properties of earthquakes [7–10], seismic electric signals [1,8,11–14], which are low-frequency electric signals that precede [15,16] earthquakes, as well as for the determination of the occurrence time of strong earthquakes [7,8,10,12,13,17–19], for a review see [20].

Chief among the advantages of using natural time analysis are the following two: First, the analysis of seismic electric signals activities revealed that natural time can identify when the system approaches criticality through the conditions

$$\kappa_1 = 0.070 \tag{1}$$

and

$$S, S_- < S_u = \frac{\ln 2}{2} - \frac{1}{4}, \tag{2}$$

where κ_1 stands for the variance of natural time and S, S_- for the entropy and the entropy under time reversal in natural time that will be discussed later. S_u stands for the entropy of a "uniform" distribution in natural time, see below. Second, the analysis of seismicity in natural time results in a universal curve for earthquakes which interestingly exhibits [7] over four orders of magnitude features similar with those obtained in several equilibrium critical phenomena [21–23] (*e.g.*, two dimensional Ising model) as well as in non-equilibrium systems [24–26] (*e.g.*, three-dimensional turbulent flow).

To obtain the universal curve for seismicity, one has to define [7] an order parameter of seismicity, which is the quantity κ_1 (see also below), and study the order parameter fluctuations relative to the standard deviation of its distribution $P(\kappa_1)$. This analysis led to the conclusion [7] that the scaled distributions for various seismic regions as well as for the worldwide seismicity (*e.g.*, see the red open circles in fig. 1) collapse on the same curve (universal). The term scaled distribution stands for $\sigma(\kappa_1)P\{[\kappa_1 - \mu(\kappa_1)]/\sigma(\kappa_1)\}$, where $\mu(\kappa_1)$ and $\sigma(\kappa_1)$ denote the average value and the standard deviation of the κ_1 values. Such a behavior is stikingly reminiscent of the one found earlier in the analysis of non-stationary biological signals including heart rate [27], locomotor activity [28] etc, where the distributions obtained for different scales of observation fall onto a single master curve.

Recently, it has been shown [19] that the value $\kappa_1 = 0.070$ can be considered as quantifying the extent of the

(a) E-mail: pvaro@otenet.gr

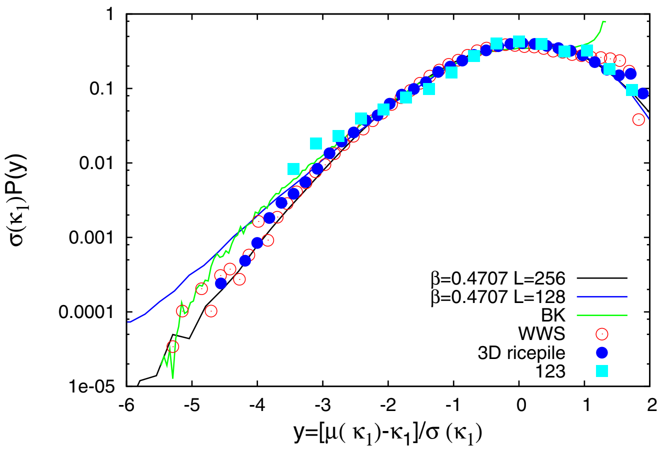

Fig. 1: (Color online) The scaled distribution $\sigma(\kappa_1)P(y)$ *vs.* $y=(\mu(\kappa_1)-\kappa_1)/\sigma(\kappa_1)$ for the BK SOC system (green) with $L=1024$ sites together with the corresponding curves for the 3D ricepile (solid blue circles) and the $YBa_2Cu_3O_{7-x}$ (cyan squares) experimental data. The red open circles correspond to the worldwide seismicity as reported in ref. [7], whereas the black (blue) solid lines correspond to the scaled distribution of the order parameter for the 2D Ising model of linear dimension $L=256(128)$ at (inverse temperature parameter) $\beta=0.4707$, which have been shown [22] to share a similar exponential tail with the corresponding curves for the 2D XY, 3D Ising and the 2D three-state Potts model. They have been drawn as a guide to the eye.

organization of a complex system at the onset of the critical stage [19]. This conclusion was drawn by analyzing in natural time, a simple deterministic SOC system [29,30] introduced to describe avalanches in stick-slip phenomena which belongs to the same universality class as the train model for earthquakes introduced by Burridge and Knopoff [31]. Here, we investigate whether the characteristic exponential tail found in the universal curve of seismicity (see fig. 1) as well as the conditions of eq. (2) are satisfied for SOC systems. For this purpose, both theoretical and experimental data are analyzed. In particular, the theoretical data come from the SOC model studied in ref. [19] (this, for the sake of convenience, will be hereafter labeled BK SOC system). As for the experimental data, we make use of the recent well-controlled experiments performed in refs. [32,33] on three-dimensional (3D) ricepiles as well as on the measurements on a thin film of $YBa_2Cu_3O_{7-x}$ reported in ref. [34]. The ricepiles are very close to the prototype [35] sandpile model of SOC, *e.g.*, see refs. [32,33,36,37], whereas the critical state in superconductors has been proposed (*e.g.*, see ref. [38]) to be a SOC system in view of the following strong analogy between sandpiles and superconductors. As first pointed out by de Gennes [39], when a type-II superconductor is put in a slowly ramped external field, magnetic vortices start to penetrate the sample from its edges. These vortices get pinned by crystallographic defects (*e.g.*, dislocations), leading to the build-up of a flux gradient which is only marginally stable in a similar fashion as is the slope in a slowly growing sandpile. Hence, it can happen that small changes in the applied field can result in large rearrangements of flux in the sample, known as flux avalanches [40–42]. Natural time analysis of the avalanches in these two experimental systems has been performed in ref. [43] (on the basis of the measurements reported in ref. [37] for ricepiles and in ref. [34] for the thin films of $YBa_2Cu_3O_{7-x}$) which led to the following conclusions: Both systems obey eq. (1) and their entropy S in natural time is smaller than the entropy S_u if a reasonable estimation error is adopted. No investigation of the entropy S_- under time reversal has been attempted at that time.

Natural time analysis. Background. – Let us now briefly summarize the natural time analysis employed here. In a time-series comprising of N avalanches the *natural time* $\chi_k=k/N$ serves as an index [1] for the occurrence of the k-th avalanche. The evolution of the pair $(\chi_k,\ Q_k)$, where Q_k is the size of the avalanche, is studied [7,8,12,43] by means of the normalized power spectrum given by

$$\Pi(\omega)=\left|\sum_{k=1}^{N}p_k\exp\left(i\omega\frac{k}{N}\right)\right|^2, \tag{3}$$

where p_k stands for $p_k=Q_k/\sum_{n=1}^{N}Q_n$, $\omega=2\pi\phi$ and ϕ denotes the *natural frequency*. In natural time analysis the properties of $\Pi(\omega)$ or $\Pi(\phi)$ are studied [7] for natural frequencies ϕ less than 0.5. This is so, because in this range of ϕ, $\Pi(\omega)$ or $\Pi(\phi)$ reduces to a kind of *characteristic function* for the probability distribution p_k in the context of probability theory, *e.g.*, see ref. [20]. According to the probability theory, the moments of a distribution and hence the distribution itself can be approximately determined once the behavior of the characteristic function of the distribution is known around zero. For $\omega\to 0$, eq. (3) leads to [1,7]

$$\Pi(\omega)\approx 1-\kappa_1\omega^2, \tag{4}$$

where κ_1 is the variance of χ given by

$$\kappa_1=\sum_{k=1}^{N}p_k\chi_k^2-\left(\sum_{k=1}^{N}p_k\chi_k\right)^2. \tag{5}$$

It has been proposed [7] that the quantity $\Pi(\omega)$ for $\omega\to 0$ (or κ_1) can be considered as an order parameter for seismicity since its value changes abruptly when a main shock occurs (cf. in this case the quantity Q_k for an earthquake is considered proportional to the energy released during the earthquake, *e.g.*, see refs. [7,10,19]). It has been shown [1] that the seismic electric signals activities (critical dynamics) have spectra $\Pi(\omega)$ that in the region $0<\phi<0.5$ scatter around

$$\Pi(\omega)=\frac{18}{5\omega^2}-\frac{6\cos\omega}{5\omega^2}-\frac{12\sin\omega}{5\omega^3}, \tag{6}$$

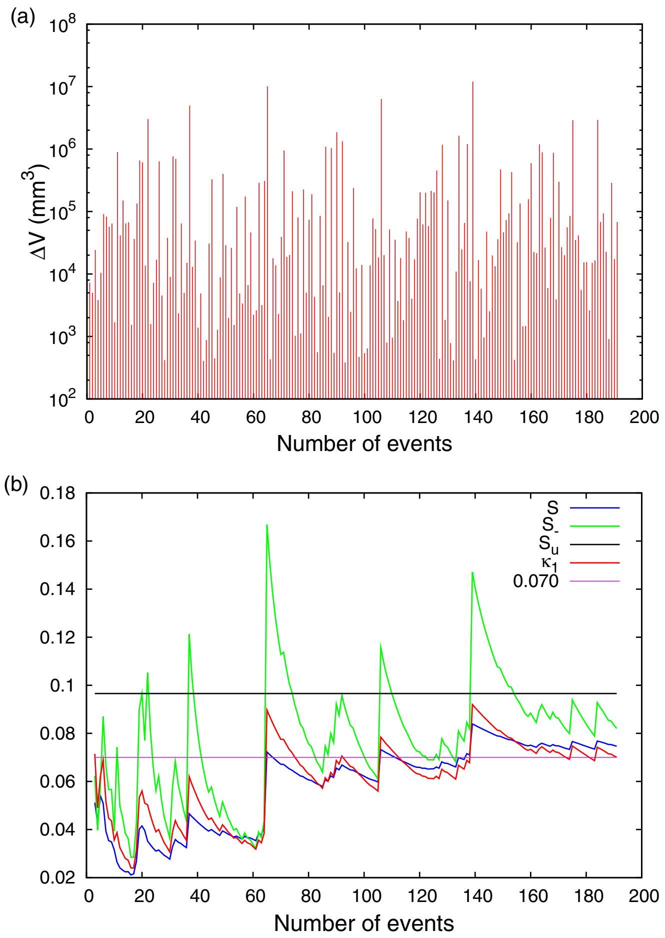

Fig. 2: (Color online) (a) The avalanches measured in ref. [33] (see their fig. 5.1) as a three-dimensional ricepile approaches the critical state. (b) The values of the entropy S (blue) and the entropy under time reversal S_- (green) in natural time as a function of the number of avalanches shown in (a). The horizontal black line corresponds to S_u. For the reader's convenience, the values of κ_1 (red) as well the value $\kappa_1 = 0.070$ (magenta) —quantifying [19] the extent of the organization of a complex system at the onset of the critical stage— are also shown.

which can be proven on the basis that the system is at criticality (for a detailed proof see ref. [20]). Equation (6) leads to a κ_1 value which is equal to 0.070, being smaller than the κ_1 value $\kappa_u = 1/12 \approx 0.0833$ that corresponds to a "uniform" distribution [6], *e.g.*, when Q_k are independent and identically distributed random variables.

The entropy S in natural time is defined [6] as

$$S = \sum_{k=1}^{N} p_k \chi_k \ln \chi_k - \left(\sum_{k=1}^{N} p_k \chi_k \right) \ln \left(\sum_{k=1}^{N} p_k \chi_k \right) \qquad (7)$$

and corresponds [6,20] to the value at $q=1$ of the derivative of the fluctuation function $F(q) = \langle \chi^q \rangle - \langle \chi \rangle^q$ with respect to q (while κ_1 corresponds to $F(q)$ for $q=2$). It is *dynamic* entropy depending on the *sequential* order of pulses [3,12]. The entropy obtained upon considering [11]

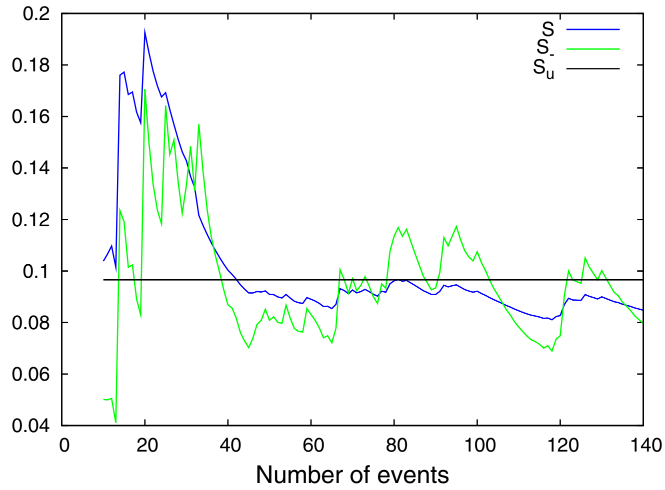

Fig. 3: (Color online) The values of the entropy S (blue) and the entropy under time reversal S_- (green) in natural time as a function of the number of events for the magnetic flux avalaches measured in a typical experiment [34] on $YBa_2Cu_3O_{7-x}$. The horizontal black line corresponds to S_u.

the time reversal $\mathcal{T}$, *i.e.*, $\mathcal{T} p_m = p_{N-m+1}$, is labelled by S_-. It was found [11] that, in general, S_- is different from S, and hence S shows the breaking of the time reversal symmetry. We note that when considering a small increasing trend $\epsilon(>0)$ for p_k *vs.* k, via the parametric family [12]

$$p(\chi;\epsilon) \equiv 1 + \epsilon(\chi - 1/2), \qquad (8)$$

so that the corresponding entropy in natural time is given by

$$S(\epsilon) \equiv \int_0^1 p(\chi;\epsilon)\chi \ln \chi \mathrm{d}\chi - \left[\int_0^1 p(\chi;\epsilon)\chi \mathrm{d}\chi \right] \times \ln \left[\int_0^1 p(\chi;\epsilon)\chi \mathrm{d}\chi \right], \qquad (9)$$

we find [12]

$$S(\epsilon) = -\frac{1}{4} + \frac{\epsilon}{72} - \left(\frac{1}{2} + \frac{\epsilon}{12} \right) \ln \left(\frac{1}{2} + \frac{\epsilon}{12} \right). \qquad (10)$$

Expanding eq. (10) around $\epsilon = 0$, we obtain that

$$S(\epsilon) = S_u + \left(\frac{6 \ln 2 - 5}{72} \right) \epsilon + O(\epsilon^2), \qquad (11)$$

where $S_u \equiv \frac{\ln 2}{2} - \frac{1}{4} \approx 0.0966$ is the entropy of the "uniform" distribution. Since $S_-(\epsilon)$ simply equals $S(-\epsilon)$, we observe that an *increasing* trend in $p(\chi;\epsilon)$, *i.e.*, $\epsilon > 0$, corresponds to $S_-(\epsilon)$ values *higher* than $S(\epsilon)$.

Data analysis and discussion. – In a time-series of avalanches comprising W events, the following procedure was followed: Starting from the first avalanche, we calculate the κ_1 values using $N = 6$ to 40 consecutive events (including the first one). We next turn to the second

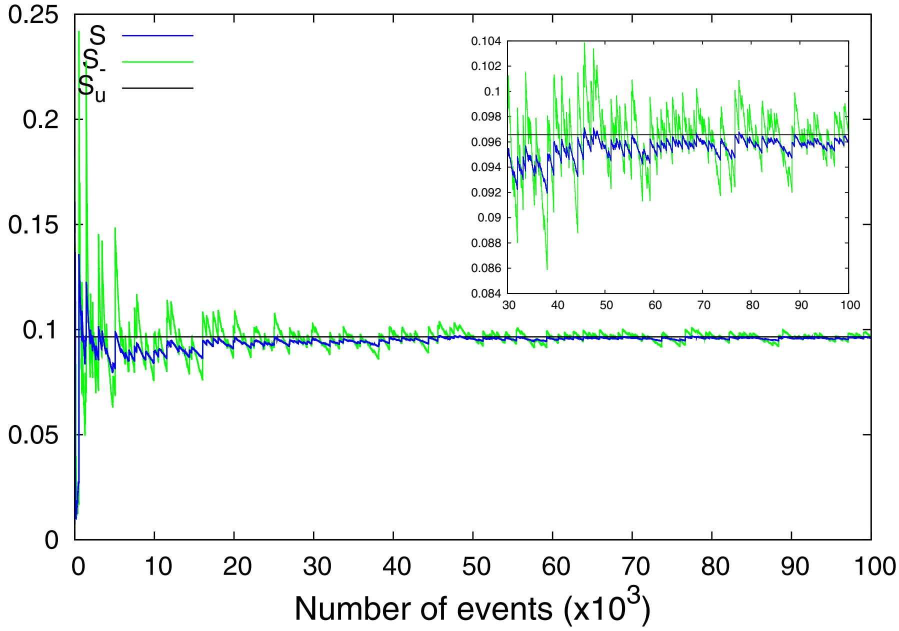

Fig. 4: (Color online) The values of the entropy S (blue) and the entropy under time reversal S_- (green) in natural time as a function of the number of avalanches for the BK SOC system with $L = 1024$ sites. The horizontal black line corresponds to S_u. For the reader's convenience, the inset shows the excerpt $N > 30 \times 10^3$ in an expanded scale.

avalanche, and repeat the calculation of κ_1. After sliding, event by event, through the whole time-series, the calculated κ_1 values enable the construction of the probability density function $P(\kappa_1)$. As mentioned, the study of the scaled distribution $\sigma(\kappa_1)P(y)$ *vs.* $y = [\kappa_1 - \mu(\kappa_1)]/\sigma(\kappa_1)$ for the long-term seismicity has revealed [7] an exponential tail similar to that obtained upon studying the order parameter fluctuations for several equilibrium and nonequilibrium systems. In fig. 1, we reproduce with red open circles the scaled distribution obtained [7] from the worldwide seismicity together with that obtained from finite-size 2D Ising systems [21–23]. We now plot in the same figure, the scaled distributions obtained from the three SOC systems investigated here: First, the green curve in fig. 1 corresponds to the results obtained from the BK SOC system. It has been obtained by analyzing time-series of $W = 10^5$ avalanches when a system of $L = 1024$ sites is *at* SOC (note that in order to examine the reliability —in the sense suggested in ref. [44]— that the same holds for other values of L, we examined the probability that the scaled distribution for $L = 512$ and $L = 4096$ could originate from the same set as the one for $L = 1024$; according to the u-test of independence of two samples performed by means of ref. [45], the corresponding probabilities are 48% and 70%, respectively, pointing to the conclusion that more or less the green curve in fig. 1 does not practically depend on L). We observe that for at least three orders of magnitude the scaled distribution for the BK SOC system *exhibits an "exponential tail" similar to that observed for the other correlated systems.* The latter tail is of profound importance, as already mentioned in refs. [7,24], since it shows that the probability for a rare fluctuation being greater from the mean by five standard deviations, is orders of magnitude higher than in the Gaussian case. Second, the solid blue circles in fig. 1 show the results for $W = 1321$ avalanches of three-dimensional ricepiles at criticality (measured in ref. [33], *e.g.*, see their fig. 4.2). An inspection of these results reveals that, at least for two orders of maginitude, the characteristic exponential tail is again present. Third, the cyan squares in fig. 1, which result from the analysis of the time-series of the magnetic flux avalanches ($W = 140$) measured [34] in a thin film of $YBa_2Cu_3O_{7-x}$, seem to scatter ("wander") around the exponential tail found in the other two SOC systems.

In what remains, we examine whether the conditions of eq. (2) hold for the SOC systems under study. Figure 2(b) depicts the values of S and S_- as a function of the number of consecutive avalanches N shown in fig. 2(a). The latter were measured in ref. [33] (see their fig. 5.1) as a three-dimensional ricepile gets progressively closer to SOC. We observe that S_- is *systematically larger* than S. This reflects that on the average the size of avalanches increases as the system approaches SOC, thus being more or less in agreement with the behavior expected from eq. (11). Moreover, if we study the values of S and S_- for $N > 65$ —which corresponds to the convenional time ($t = 2.4 \times 10^4$ s) identified in ref. [33] as the time at which the system enters the critical state— we find that the average value (standard deviation) of S is $S = 0.070(6)$ whereas the corresponding value for the entropy under time reversal is $S_- = 0.089(18)$. Thus, returning to the relation (2), it seems that although the condition $S < S_u$ is systematically obeyed, the other condition $S_- < S_u$ is *only* marginally valid as it is violated roughly for 25% of the data. Note that κ_1 results in $\kappa_1 = 0.070(8)$, hence being in accordance with eq. (1) as well as with the κ_1 value, $\kappa_1 = 0.07(1)$, reported in ref. [43].

Figure 3 depicts how the values of S and S_- vary when the magnetic flux avalanches measured by Aegerter *et al.* [34] in a thin film of $YBa_2Cu_3O_{7-x}$ are analyzed in natural time. Notice that Aegerter *et al.* [34] measured the magnetic flux avalanches after the steady SOC state had been reached, thus the situation essentially *differs* from that in the 3D ricepile data of fig. 2(a). Actually, we now find that the systematic excess of S_- compared to S, found in fig. 2(b), is absent. This is so, because in $YBa_2Cu_3O_{7-x}$ we observe that it is unclear which of the two quantities S or S_- is larger, which may reflect that stationarity has been reached. This is fortified by the fact that the u-test of independence of the two samples of S and S_- made using the software of ref. [45] resulted in 24% probability that S and S_- come from the same random set. Moreover, if we study the values of S and S_- (for $N > 40$ so that to minimize the initial variation due to the small number of avalanches N), we find that the average values (standard deviations) result in $S = 0.090(4)$ and $S_- = 0.090(13)$. Thus, the conditions of the relation (2) are marginally satisfied for this system *at* SOC.

We now finally examine the validity of eq. (2) in the case of the avalanches obtained from the BK SOC system. The results obtained are shown in fig. 4. We observe that in this case the average values obtained together with the standard deviations in parentheses are $S = 0.094(6)$ and $S_- = 0.096(9)$. Hence, both S and S_- are very close to the value S_u of the "uniform" distribution, thus they only marginally satisfy the conditions of eq. (2).

Conclusions. – In summary, the time-series of avalanches have been analyzed in natural time in three systems that exhibit SOC. In two of them, *i.e.*, ricepiles and magnetic flux penetration in type-II superconductors, the data come from laboratory measurements, while the third one is a deterministic model mimicking stick-slip phenomena. The main conclusions are: First, their scaled distributions for the variance κ_1 of natural time share —at least over two orders of magnitude— an exponential tail already observed for the scaled distribution of the order parameter of seismicity as well as for the corresponding distributions of other equilibrium and non-equilibrium critical systems like 2D Ising model and 3D turbulence. Second, in all three SOC systems investigated, their entropy S in natural time seems to be smaller than that of the "uniform" distribution. Third, concerning the entropy S_- under time reversal, the following important difference emerges: In ricepiles (see fig. 2(b)), S_- is systematically larger than S, which probably reflects that the system is still *evolving towards* the SOC state, while in the $YBa_2Cu_3O_{7-x}$ case —which has already reached the SOC state— no systematic difference between S_- and S is found. The latter behavior is also observed for the deterministic model mimicking stick-slip phenomena studied here, *i.e.*, the BK SOC model. As for the S_- value itself, the condition $S_- < S_u$ should be considered with care, since it may be violated in some cases. Even in such cases, however, a safe upper bound of S_- does not seem to differ from S_u more than 30%, leading to $S_- < 1.3S_u$.

* * *

We express our sincere thanks to Prof. R. J. Wijngaarden for sending us the $YBa_2Cu_3O_{7-x}$ data and to Dr. K. A. Lőrincz for kindly providing the ricepile data analyzed.

REFERENCES

[1] Varotsos P. A., Sarlis N. V. and Skordas E. S., *Phys. Rev. E*, **66** (2002) 011902.
[2] Abe S., Sarlis N. V., Skordas E. S., Tanaka H. K. and Varotsos P. A., *Phys. Rev. Lett.*, **94** (2005) 170601.
[3] Varotsos P. A., Sarlis N. V., Skordas E. S. and Lazaridou M. S., *Phys. Rev. E*, **71** (2005) 011110.
[4] Varotsos P. A., Sarlis N. V., Skordas E. S. and Lazaridou M. S., *Appl. Phys. Lett.*, **91** (2007) 064106.
[5] Sarlis N. V., Skordas E. S. and Varotsos P. A., *EPL*, **87** (2009) 18003.
[6] Varotsos P. A., Sarlis N. V. and Skordas E. S., *Phys. Rev. E*, **68** (2003) 031106.
[7] Varotsos P. A., Sarlis N. V., Tanaka H. K. and Skordas E. S., *Phys. Rev. E*, **72** (2005) 041103.
[8] Varotsos P. A., Sarlis N. V., Skordas E. S., Tanaka H. K. and Lazaridou M. S., *Phys. Rev. E*, **74** (2006) 021123.
[9] Sarlis N. V., Skordas E. S. and Varotsos P. A., *Phys. Rev. E*, **80** (2009) 022102.
[10] Sarlis N. V., Skordas E. S. and Varotsos P. A., *EPL*, **91** (2010) 59001.
[11] Varotsos P. A., Sarlis N. V., Tanaka H. K. and Skordas E. S., *Phys. Rev. E*, **71** (2005) 032102.
[12] Varotsos P. A., Sarlis N. V., Skordas E. S., Tanaka H. K. and Lazaridou M. S., *Phys. Rev. E*, **73** (2006) 031114.
[13] Varotsos P. A., Sarlis N. V. and Skordas E. S., *Chaos*, **19** (2009) 023114.
[14] Skordas E. S., Sarlis N. V. and Varotsos P. A., *Chaos*, **20** (2010) 033111.
[15] Varotsos P. and Alexopoulos K., *Tectonophysics*, **110** (1984) 73.
[16] Varotsos P. and Alexopoulos K., *Tectonophysics*, **110** (1984) 99.
[17] Sarlis N. V., Skordas E. S., Lazaridou M. S. and Varotsos P. A., *Proc. Jpn. Acad., Ser. B*, **84** (2008) 331.
[18] Uyeda S., Kamogawa M. and Tanaka H., *J. Geophys. Res.*, **114** (2009) B02310.
[19] Varotsos P. A., Sarlis N. V., Skordas E. S., Uyeda S. and Kamogawa M., *EPL*, **92** (2010) 29002.
[20] Varotsos P., Sarlis N. and Skordas E., *Natural Time Analysis: The New View of Time* (Springer-Verlag, Berlin, Heidelberg) 2011.
[21] Zheng B. and Trimper S., *Phys. Rev. Lett.*, **87** (2001) 188901.
[22] Zheng B., *Phys. Rev. E*, **67** (2003) 026114.

[23] Clusel M., Fortin J.-Y. and Holdsworth P. C. W., *Phys. Rev. E*, **70** (2004) 046112.
[24] Bramwell S. T., Holdsworth P. C. W. and Pinton J. F., *Nature* (*London*), **396** (1998) 552.
[25] Bramwell S. T., Christensen K., Fortin J.-Y., Holdsworth P. C. W., Jensen H. J., Lise S., López J. M., Nicodemi M., Pinton J.-F. and Sellitto M., *Phys. Rev. Lett.*, **84** (2000) 3744.
[26] Bramwell S. T., Fortin J.-Y., Holdsworth P. C. W., Peysson S., Pinton J.-F., Portelli B. and Sellitto M., *Phys. Rev. E*, **63** (2001) 041106.
[27] Ivanov P. C., Rosenblum M. G., Peng C. K., Mietus J., Havlin S., Stanley H. E. and Goldberger A. L., *Nature*, **383** (1996) 323.
[28] Hu K., Ivanov P. C., Chen Z., Hilton M. F., Stanley H. E. and Shea S. A., *Physica A*, **337** (2004) 307.
[29] de Sousa Vieira M., *Phys. Rev. E*, **61** (2000) R6056.
[30] Davidsen J. and Paczuski M., *Phys. Rev. E*, **66** (2002) 050101.
[31] Burridge R. and Knopoff L., *Bull. Seismol. Soc. Am.*, **57** (1967) 341.
[32] Lőrincz K. A. and Wijngaarden R. J., *Phys. Rev. E*, **76** (2007) 040301.
[33] Lőrincz K. A., *Avalanche dynamics in a three-dimensional pile of rice,* PhD Thesis, Vrije Universiteit (Gildeprint Drukkerijen Enschede, Amsterdam, The Netherlands) 2008.
[34] Aegerter C. M., Welling M. S. and Wijngaarden R. J., *Europhys. Lett.*, **65** (2004) 753.
[35] Bak P., Tang C. and Wiesenfeld K., *Phys. Rev. Lett.*, **59** (1987) 381.
[36] Aegerter C. M., Gunther R. and Wijngaarden R. J., *Phys. Rev. E*, **67** (2003) 051306.
[37] Aegerter C. M., Lorincz K. A., Welling M. S. and Wijngaarden R. J., *Phys. Rev. Lett.*, **92** (2004) 058702.
[38] Zaitsev S. I., *Physica A*, **189** (1992) 411.
[39] de Gennes P. G., *Superconductivity of Metals and Alloys* (Addison-Wesley, New York) 1966.
[40] Campbell A. M. and Evetts J. E., *Adv. Phys.*, **50** (2001) 1249.
[41] Altshuler E. and Johansen T. H., *Rev. Mod. Phys.*, **76** (2004) 471.
[42] Welling M. S., Aegerter C. M. and Wijngaarden R. J., *Phys. Rev. B*, **71** (2005) 104515.
[43] Sarlis N. V., Varotsos P. A. and Skordas E. S., *Phys. Rev. B*, **73** (2006) 054504.
[44] Huang Qinghua, *J. Geophys. Res.*, **111** (2006) B04301.
[45] Melcher D., Computer code STATIST, available from `http://www.usf.uos.de/~breiter/tools/statist/index.en.html` (2001).